Check for updates

Radio pulsations from a neutron star within the gamma-ray binary LS I +61° 303

Shan-Shan Weng [1,14] ✉, Lei Qian [2,3,14], Bo-Jun Wang[2,4,5,14], D. F. Torres [6,7,8] ✉, A. Papitto[9], Peng Jiang[2,3], Renxin Xu[4,5], Jian Li [10,11], Jing-Zhi Yan[12], Qing-Zhong Liu[12], Ming-Yu Ge[13] and Qi-Rong Yuan[1]

LS I +61° 303 is one of the rare gamma-ray binaries[1] that emit most of their luminosity in photons with energies beyond 100 MeV (ref. [2]). It is well characterized—the ~26.5 day orbital period is clearly detected at many wavelengths[2-4]—and other aspects of its multifrequency behaviour make it the most interesting example of its class. The morphology of high-resolution radio images changes with orbital phase, displaying a cometary tail pointing away from the high-mass star component[5] and LS I +61° 303 also shows superorbital variability[3,6-9]. A couple of energetic (~10^{37} erg s^{-1}), short, magnetar-like bursts have been plausibly ascribed to it[10-13]. Although the phenomenology of LS I +61° 303 has been the subject of theoretical scrutiny for decades, there has been a lack of certainty regarding the nature of the compact object in the binary that has hampered our understanding of the source. Here, using observations with the Five-hundred-meter Aperture Spherical radio Telescope, we report the existence of transient radio pulsations from the direction of LS I +61° 303 with a period $P = 269.15508 \pm 0.00016$ ms at a significance of >20σ. These pulsations strongly argue for the existence of a rotating neutron star within LS I +61° 303.

LS I +61° 303 is located at a distance of 2.65 ± 0.09 kpc (ref. [14]) and contains a compact object orbiting a rapidly rotating B0Ve star every 26.5 days (refs. [3,15]). The dynamical mass of the compact object is between 1 and 4 solar masses ($M_\odot$); thus, from dynamical arguments alone, it could either be a neutron star or a low-mass black hole[15-17]. Models involving an accreting black hole launching a relativistic jet (a microquasar; see for example, ref. [18]), a rotationally powered neutron star emitting a relativistic wind of particles in interactions with the stellar wind of the companion[19] and a neutron star alternating between rotationally powered emission and propeller ejection of the mass lost by the companion[20] have been proposed to explain the multifrequency phenomenology. Despite the ability of modern incarnations of these models to provide a framework with which to interpret the growing number of observations, the fact that they are based on dissimilar compact object scenarios stagnated progress.

Previous deep searches in the radio[21,22], X-ray[23] and gamma-ray bands[24] did not find pulsations. This is in fact not surprising: free–free absorption—which may have a complex temporal behaviour depending on the binary conditions—can easily wash out the pulses in the radio band; see for example ref. [25]. The radio cone of the emission may also point in a completely different direction than Earth. In the X-ray band, the imposed pulsed fraction upper limit of ~10% (at a 3σ confidence level) could well be larger than the actual pulsed fraction of the source, as is the case for other pulsars. In fact, non-thermal X-ray pulsations have been detected in only a few dozen of the roughly 300 detected pulsars in the gamma-ray band and approximately 3,000 in the radio band. Finally, in the gamma-ray band, LS I +61° 303 lies in a complex and populated region, and the diffuse background, in addition to the likely origin of at least part of the gigaelectronvolt emission beyond the magnetosphere of the putative pulsar, may preclude the detection of pulses. The relatively large uncertainty in the orbital parameters also reduces the sensitivity of blind searches across all frequencies when long integration times are needed[26]. The best chance of detecting pulsations from LS I +61° 303 was offered by observing it with a high radio sensitivity in the orbital region where the free–free absorption effect due to the stellar wind (or disk) would naturally be the lowest[22].

The Five-hundred-meter Aperture Spherical radio Telescope (FAST) is the largest single-aperture radio telescope, and is located in a naturally deep and round karst depression in southwest China's Guizhou province (Methods). FAST executed four observations towards LS I +61° 303, with a total exposure time of ~10.2 h (Table 1): one at an orbital phase of ~0.07 and three around an orbital phase of ~0.6. The 0 orbital phase of LS I +61° 303 is defined in modified Julian days (MJD) as $\text{MJD}_0 = 43{,}366.275$, and the orbital period is estimated to be $P = 26.4960$ days (for example, see ref. [3]). In quoting orbital phases, we have assumed that the orbital phase of periastron is $\phi_\text{peri} = 0.23$ (ref. [17]), as is widely assumed in the study of this source (but see Methods for further discussion of orbital uncertainties).

The pulsar exploration and search toolkit (PRESTO) package[27] was used to search for the periodic signal. The dispersion measure in the direction of LS I +61° 303 as predicted by the YMW16 model[28] is 138.58 pc cm^{-3}, whereas its upper limit is 316.59 pc cm^{-3}.

[1]Department of Physics and Institute of Theoretical Physics, Nanjing Normal University, Nanjing, China. [2]National Astronomical Observatories, Chinese Academy of Sciences, Beijing, China. [3]CAS Key Laboratory of FAST, National Astronomical Observatories, Chinese Academy of Sciences, Beijing, China. [4]Kavli Institute for Astronomy and Astrophysics, Peking University, Beijing, China. [5]Department of Astronomy, School of Physics, Peking University, Beijing, China. [6]Institució Catalana de Recerca i Estudis Avançats (ICREA), Barcelona, Spain. [7]Institute of Space Sciences (ICE, CSIC), Barcelona, Spain. [8]Institut d'Estudis Espacials de Catalunya (IEEC), Barcelona, Spain. [9]INAF-Osservatorio Astronomico di Roma (OAR), Rome, Italy. [10]CAS Key Laboratory for Research in Galaxies and Cosmology, Department of Astronomy, University of Science and Technology of China, Hefei, China. [11]School of Astronomy and Space Science, University of Science and Technology of China, Hefei, China. [12]Key Laboratory of Dark Matter and Space Astronomy, Purple Mountain Observatory, Chinese Academy of Sciences, Nanjing, China. [13]Key Laboratory of Particle Astrophysics, Institute of High Energy Physics, Chinese Academy of Sciences, Beijing, China. [14]These authors contributed equally: Shan-Shan Weng, Lei Qian, Bo-Jun Wang. ✉e-mail: wengss@njnu.edu.cn; dtorres@ice.csic.es

Table 1 | Observational log

Middle of observation time	Orbital phase	Exposure time (h)	Sampling time (μs)	Pulse detected	S_{mean} (μJy)	S_{UL} (μJy)
58,788.7257	0.07	2.2	98.304	No	–	1.61
58,855.5278	0.59	3.0	98.304	Yes	4.40	1.37
59,093.8646	0.58	3.0	196.608	No	–	1.37
59,094.8681	0.62	2.0	196.608	No	–	1.68

The orbital phases are calculated with the radio ephemeris given in ref. [3]. S_{mean}, mean flux density for detection; S_{UL}, upper limit of the flux density; –, mean flux density for non-detection.

To avoid missing the signal, and taking into account the error, the range of dispersion measures used for our search was 0–500 pc cm^{-3}. As the orbital period is much longer than the exposure time, the Doppler effect is negligible. We carried out the acceleration search with the max number of Fourier bins, zmax = 200, we also used the Burst Emission Automatic Roger routine to search for single pulses (see details in the Methods).

An unambiguous pulse signal (a single-trial significance of ~22.4σ; Methods) with a single-peak profile emerged from the data taken on 2020 January 7 (MJD = 58,855.5278; Fig. 1). The period, pulse width and dispersion measure of this pulsar are 269.15508 ± 0.00016 ms, 33.30 ± 0.96 ms and 240.1 pc cm^{-3}, respectively (see also Supplementary Fig. 1). The pulsations disappeared in the third and fourth observations (taken 1 day apart), which were taken several months after the positive detection, at a similar orbital phase. A single-pulse search was conducted for our observations; more than 40 were detected in the second observation (where the radio pulsation is visible), but none were seen in the other three (Methods).

Given that our observations are short in comparison to the orbital period of the binary, and that the pulsation seems to be non-steady in nature, the orbital imprint cannot be detected in our data. In addition, the angular resolution (L-band) of FAST is ~2.9′. As for other FAST observations in the same band, we cannot therefore formally exclude the presence of a pulsar just behind LS I +61° 303, unrelated to it, that is responsible for the pulsed emission. This is deemed unlikely, however (Methods).

The fact that the pulsations are not present in three out of four observations (a couple of which are very close to one another) reveals a rapid change in conditions in the interstellar medium between us and the source, in the neutron star environment or in the neutron star itself.

Interstellar scintillation may be produced by a diffractive scattering medium along our line of sight, for which the typical diffractive interstellar scintillation timescale[29] is $\Delta t_{\rm d} = 2.53 \times 10^4 (D \Delta \nu_{\rm d})^{1/2}/(\nu V_{\rm ISS})$ s, where D is the distance to the source in kiloparsecs, $\Delta \nu_{\rm d}$ is the decorrelation bandwidth in megahertz, ν is the observed frequency in gigahertz and $V_{\rm ISS}$ the velocity of interstellar scintillation diffraction pattern (in km s^{-1}; in binaries this is typically dominated by pulsar velocities, in the range of a few tens to a few hundred km s^{-1}). For the observation shown in Fig. 1, scintillation could explain changes in flux up to a few minutes, but not several hours, in consecutive days when pulsations are absent. And this does not take into account that the bandwidth of the observation is wider than the decorrelation bandwidth, and therefore scintillation would be averaged out. Refractive scintillation, on the other hand, could have a longer timescale and we cannot rule it out a priori, although the flux modulation we have seen would be larger than expected[30].

A second possibility is that the flux modulation is related to an intrinsic nulling of the pulsar: a temporary broadband cessation of normal pulsar emission, probably produced by magnetospheric changes. About 8% of known pulsars exhibit nulling[31], with durations

that range from a single pulse to several days. Some pulsars are actually in this null state most of the time, and are active for only short periods, making them difficult to detect. Mode changing is a related phenomenon where the mean pulse profile abruptly changes in a matter of minutes to revert to the original later on (see, for example, ref. [32]). With the current lack of information regarding pulsations at other frequencies, it is not possible to associate the absence of pulsations we observed with nulling or mode changing. The fairly rapid spin period, and the plausibly low age of LS I +61° 303 (see, for example, ref. [1]), may argue against these interpretations. Nulling appears predominantly in longer-period and older pulsars. It is interesting, in the same context, to note the similarity of the phenomenology seen to observations of rotating radio transients, pulsars that sporadically emit single-pulse outbursts instead of continuous pulse trains[33].

Finally, changes in the stellar wind properties can easily affect the pulsed signal. And as the Be stellar wind is likely to be clumpy, it would be impossible to predict the absorption level that any radio signal would be subject to on a local basis (see the discussion in ref. [25]). The transient behaviour could thus plausibly be interpreted as a result of the rapid change in the environmental conditions. Regarding this possibility, it might be useful to compare observations with the case of the pulsar-composed gamma-ray binary PSR B1259-63. Despite this system having a much larger orbit, radio flux variations at a timescale of minutes to hours were also reported in PSR B1259-63, together with changes in the local properties of the Be stellar wind/disk encountered by the pulsar (see for example ref. [34] and references therein). It is reasonable to expect these same effects to apply to LS I +61° 303, enhanced by the smaller spatial scale of the system.

We can also draw some phenomenological connections to transitional pulsars. These are redback systems: a millisecond pulsar in close orbit to a low-mass companion star. These systems can exhibit highly variable eclipses from orbit to orbit, radio variability and X-ray/radio anticorrelation, and some also fully disappear in the radio for days (see, for example ref. [35]). Although LS I +61° 303 is not a redback pulsar, it is similar in that it does have a non-compact stellar companion that fills the system with ionized gas. The variability of the pulsations could be due to the latter, and the pulsed signal can also be affected by matter–magnetosphere interactions. Future simultaneous campaigns in the X-ray and radio bands may shed further light on this comparison.

In any case, our finding suggests that LS I +61° 303 is a pulsar-composed system and place the tight constraint on pulsar-based models when explaining its multifrequency phenomenology. Among them, models based on state transitions might be appealing: a study in the context of the short magnetar-like flares and superorbital variability determined a preferred pulsar period for LS I +61° 303 of 0.26 s (see fig. 4 of ref. [36]), as we find here. With the knowledge gained from our observational finding, this and other pulsar-based models can be revisited and enhanced, and applied to the search and characterization of pulsations at all frequencies.
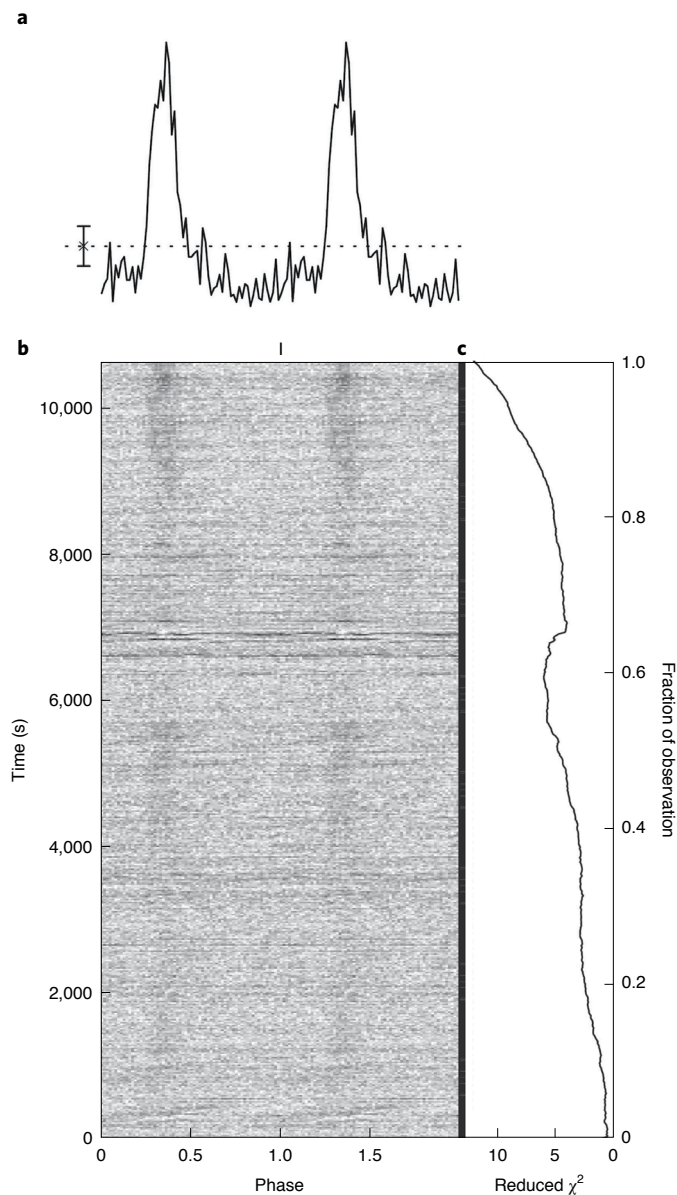
Fig. 1 | Radio pulsations were recorded in the FAST data recorded on 2020 January 7. a, Two cycles of integrated pulse profile with the best-fitted spin period. The dotted line and the asterisk mark the mean flux level of pulsed emission, and the standard deviation of the pulse profile is plotted with the error bar. **b**, Intensity of the pulse. **c**, Reduced χ^2 as a function of the pulse phase and the observational time. The data were folded over $P = 269.15508$ ms, and the reduced χ^2 (that is, the significance of the pulsation) was computed with the folded profile compared with the average value of the folded profile.

Methods

FAST observations. FAST is the most sensitive operating radio telescope[37,38], and it has recently been used to detect some very faint pulsars[39–41]. LS I +61° 303 was observed by FAST four times in 2019–2020, and all data were processed in the same way with the packages available in PRESTO using the following steps[27]: (1) we masked and zapped the radiofrequency interference (RFI) using the routine rfifind; (2) after RFI excision, the data were dedispersed with the trial dispersion measures between 0 and 500 pc cm^{-3} using the routine prepsubband; (3) for the resulting dedispersed time series, we carried out a blind Fourier-domain acceleration periodicity search with the routines realfft and accelsearch, yielding periodic candidates; (4) the periodic candidates were further sifted with the routine ACCEL_sift.py; (5) the data were corrected to the Solar System barycentre and were automatically folded over all derived periodic candidates and possible period

derivatives ($\dot{P}$) using the routine prepfold. We could then check and confirm the signal by diagnosing the folding plots. That is, the precise values of the dispersion measure, P, $\dot{P}$ and their uncertainties were obtained by folding the data to reach a maximum χ^2 (that is, SNR).

The pulsations were only detected in the FAST data taken on 2021 January 7, and the folding results with the identified $P = 269.15508 \pm 0.00016$ ms are shown in Supplementary Fig. 1. We did not find any public pointed observation around 2020 January 7 in multi-wavelength bands. We checked that there was no unusual behaviour displayed in survey data, including Swift Burst Alert Telescope (BAT), the Monitor of All-sky X-ray Image (MAXI) and Fermi Large Area Telescope (LAT).

Owing to the fact that we considered only 3 h of observations spanning a very small range of orbital phases, we could not recover the Doppler-shifted signals to determine this pulsar's intrinsic $\dot{P}$ and $\ddot{P}$. When carrying out a non-acceleration search with the option '-nopdsearchr' in the routine prepfold, we obtained a slightly smaller single-trial significance of ~21.1σ.

An estimate of the mean flux density that each of our observations would have detected, S_{mean}, can be obtained via[42]:

$$S_{mean} = \frac{\eta \beta T_{sys}}{G \sqrt{N_p \Delta\nu T_{int}}} \sqrt{\frac{W}{P - W}} \tag{1}$$

where η is the S/N threshold, β is the sampling efficiency, T_{sys} is the system temperature, T_{int} is the integration time and G is antenna gain. For FAST, $\beta = 1$, $T_{sys} = 24$ K and $G = 16$ K Jy^{-1}. The bandwidth $\Delta\nu$ was 300 MHz, as we masked 100 MHz in our pipeline due to the RFI. $N_p = 2$ was the number of polarizations and W is the width of pulse profile. The value $W/P = 0.1$ (see the figure in the main text) was adopted for LS I +61° 303. The 7σ detection limit ($\alpha = 7$) of the flux density for each observation, S_{UL}, was also calculated and is listed in Table 1.

In comparison, the Green Bank Telescope (https://greenbankobservatory.org/science/telescopes/gbt/) and the 100-m Effelsberg radio telescope (https://www.mpifr-bonn.mpg.de/effelsberg/astronomers) have similar system temperatures, but lower antenna gains, 2 K Jy^{-1} and 1.55 K Jy^{-1} at 1.4 GHz, respectively. That is, the mean pulsed signal reported with FAST data (~4.4 μJy; Table 1) would be unattainable for the Green Bank Telescope and Effelsberg telescope: an unrealistic integration time of >20–30 h would have been required for a 7σ detection. Alternatively, flux variations, as are evident in LS I +61° 303 may lead to overpassing the threshold for detection at certain times. According to equation (1), the estimated pulsed flux of LS I +61° 303 increased up to 12.85 μJy (single-trial significance of 26.7σ) in the last half hour. This level of flux might be detected by the Green Bank Telescope and Effelsberg telescope within a reasonable observational time of ~2.2 h. LS I +61° 303 is too northerly to be observed by Arecibo (http://www.naic.edu/science/generalinfo_set.htm).

Single-pulse analysis. In addition to PRESTO, we also used the package Burst Emission Automatic Roger (BEAR)[43] to conduct a single-pulse search for all observational data. The RFI in FAST data mostly comes from satellites, so frequencies from 1,200–1,240 MHz and 1,270–1,300 MHz were cut from the data. We dedispersed the data from 0 pc cm^{-3} to 500 pc cm^{-3} in steps of 0.5 pc cm^{-3} and used a box-car-shaped match filter to search for bursts with a width between 0.2 ms and 30 ms. Candidates with a SNR threshold larger than 7 were plotted by BEAR and visually inspected. For our data, the observations performed on MJD 58,788, 59,093 and 59,094 led to no significant detection in our single-pulse-searching pipeline. The analysis of the data obtained on MJD 58,855 led to 42 single pulses. Supplementary Fig. 2 shows all of the dynamic spectra and profiles of the single pulses. The parameters of all of these single pulses are listed in Supplementary Table 1. The DM value for every single pulse (DM$_{s/n}$) was obtained by aligning the signal across frequencies to achieve the best peak SNR[44]. This also explains the apparent variability seen in the dispersion measure values; however, the mean dispersion measure was 240.2 pc cm^{-3}, which is consistent with the pulsar mentioned above. We used intensity weighted width to measure the burst width by treating the pulse profile as the temporal intensity distribution function, and then calculated the standard deviation in time. The mean flux density was computed using the following equation, uncertainties are dominated by the system noise temperature (~20%; ref. [38]).

$$S_{mean} = \frac{SNR \cdot T_{sys}}{G \sqrt{N_p T_{sample} \Delta\nu}} \tag{2}$$

We show the folded single-pulse data with P and $\dot{P}$ obtained in Supplementary Fig. 1, and display their occurrences in the time–phase diagram with the red bars (Supplementary Fig. 3).

The non-zero dispersion measure value and the variable RFI recorded in the data suggested that the detected pulses were unlikely to be a result of instrumental or terrestrial interference. The single pulses also displayed dramatic flux variations (by a factor of >10³; Supplementary Table 1) over short timescales, while retaining the dispersion measure value. Therefore, the detections of both the weak averaged pulse and the energetic single pulses in the same observation cannot be interpreted as instrumental in origin or the result of terrestrial interference.

In addition, the detection of energetic single pulses would indicate that the emission is unlikely to be from the secondary lobes; that is, emission from a pulsar

far away from the field of LS I +61° 303 (~6–8′; ref. [45]). If the emission came from secondary lobes, the intrinsic flux density would be about ~10^3 times brighter than the detected level[45]; that is, ~10−100 Jy. If so, other telescopes could have easily detected the signal. While this paper was being reviewed, we made another dozen FAST observations, covering the whole orbital phase. The preliminary analysis revealed several single pulses on 2021 November 2, corresponding to an orbital phase of ~0.69. These single pulses share similar properties to those reported here in more detail and further support their origin in LS I +61° 303. A detailed analysis of these single pulses will be presented elsewhere.

Pulse number 24 and pulse number 41 show an exponential-like scattering tail. For these two bursts, we used a Gaussian convolved with a one-sided exponential function to fit them,

$$f(t, \tau) = \frac{S}{2\tau} \exp\left(\frac{\sigma^2}{2\tau^2}\right) \exp\left(-\frac{t-\mu}{\tau}\right) \times \left\{1 + \mathrm{erf}\left[\frac{t-(\mu+\sigma^2/\tau)}{\sigma\sqrt{2}}\right]\right\} \tag{3}$$

where S is the flux density of the Gaussian, μ is its centre and σ s.d. τ is a time constant of the one-sided exponential function. We split the data into 8 evenly spaced subbands across the 500 MHz raw bandwidth, then clipped the channels' RFI. For each subband with SNR ≥ 7, we integrated the pulse intensities over time and used Markov chain Monte Carlo methods to fit the intensity profile with the equation above along the frequency axis (Supplementary Figs. 4b and 5b) to obtain the scattering time scale of each subband (τ_{chn}) and the standard deviation (σ_{chn}) (Supplementary Figs. 4c and 5c). For each frequency channel, the scattering timescale is

$$\tau_{chn}(\nu) = \tau_{chn}\left(\frac{\nu}{\nu_{ref}}\right)^{\alpha} \tag{4}$$

where ν_{ref} is the reference frequency (set to 1 GHz) and α is the frequency scaling index. Linear regression of the scattering timescales showed their scattering timescales at 1 GHz to be $\tau_{1GHz} = 29.85 \pm 4.64$ ms and 15.57 ± 2.39 ms and $\alpha = -2.49 \pm 0.53$ and -1.91 ± 0.80 for the two pulses, respectively. The scattering by ionized plasma led to the pulse being asymmetrically broader at lower frequencies. For the thin-screen scattering model, we could expect scaling indexes of −4 and −4.4 for Gaussian and Kolmogorov inhomogeneities, respectively[46,47]. However, note that deviations from the theoretical models had been already reported in several pulsars (for example PSR B0823+26, PSR B1839+56 and others): it was suggested that lower α values could result from limitations of the thin-screen model or from an anisotropic scattering mechanism[48]. In our case, the distribution of the ionized plasma around LS I +61° 303 cannot be an infinite thin screen, and should deviate from either Gaussian or Kolmogorov inhomogeneous distribution.

Uncertainties. Except for the orbital period, other orbital parameters including ϕ_{peri} and the eccentricity bear relatively large uncertainties. The orbital period is now well defined as $P \approx 26.4960 \pm 0.0028$ days (see for example ref. [3]). ϕ_{peri} was estimated by fitting the radial velocities to lie in the range of 0.23–0.30, and the eccentricity e in the range of 0.55–0.72 (for example, refs. [15–17]). Recently, however, Kravtsov et al.[49] obtained a notably different orbital solution using optical polarization measurements: small $e < 0.2$ and $\phi_{peri} \approx 0.6$, although some of their parameters are degenerate. The latter solution, as the authors discussed, is not devoid of assumptions that may directly impact the results. If correct, the solution presented by Kravtsov et al. would imply that notable reassessments are needed when considering, for instance, the orbital location and interpretation of all multifrequency phenomenology of the system, as well its age. However, we advise to keep this uncertainty in mind until a final orbital solution is established beyond doubt. Given that our observations are short in comparison to the orbital period of the binary, and that the pulsation seems to be non-steady in nature, the orbital imprint cannot be constrained with our data.

Finally, we ponder how likely it could be that, within this spatial extent, FAST is actually detecting a different pulsar lying within the angular resolution (L-band) of FAST (~2.9′; ref. [38]). For LS I +61° 303 in particular, a similar issue appeared when analysing the magnetar-like flares detected from the same region[10–12]. Swift, the X-ray satellite that observed them, had an ~1.4′ positional uncertainty and no candidate different from LS I +61° 303 was found. A reanalysis of the flare data, as well as a subsequent 96 ks observation with the Chandra X-ray telescope, did not reveal a candidate in that region either[13]; nor did a combined analysis of archive Very Large Array radio data and near-infrared observations[12]. These studies concluded that the simplest explanation is that LS I +61° 303 was the origin of the flares.

There are just a few gamma-ray binaries known in the Galaxy (fewer than ten in total) and we know about 3,000 radio pulsars[50], of which about 30 have shown magnetar-flare behaviour. If we were to assume that LS I +61° 303 is different from the radio pulsar we detected, and also from the origin of the magnetar-like flares detected from the same region earlier, we would need to find three relatively rare objects aligned within a few arcmin. To qualitatively assess how likely this is, we considered first that the short bursts and the radio pulsations reported here come from two unrelated neutron stars in the small field of view close to LS I +61° 303.

Using the ATNF Pulsar Catalogue (https://www.atnf.csiro.au/research/pulsar/psrcat/) as a basis for what we have been able to detect with current instruments, taking all 2,072 pulsars within the Galactic latitude of ±10° and excluding those in globular clusters, the probability of finding two pulsars within ~2.9′ is <7×10^{-6}. We would still need to multiply this by the probability of finding LS I +61° 303 within the same region. Assuming that there are ten sources like LS I +61° 303, the probability would reduce to <1×10^{-11}. If we were to assume that the system producing the magnetar-like flare and the pulsation we detect are the same (that is, a single pulsar, but different from LS I +61° 303) the probability of randomly finding both a pulsar producing magnetar phenomenology and a gamma-ray binary within ~2.9′ assuming a uniform distribution in the ±10° Galactic plane region, would be ~3×10^{-10}.

We note that these numbers are uncertain, as they lack details regarding the non-uniform spatial distribution of sources or considerations relating to the age the system. The magnetar behaviour, for instance, seems to appear more often at younger pulsar ages, so not all pulsars would equally serve as a counterpart for the flares (see for example, ref. [51]). These estimations are also subject to biases from incomplete and non-uniform observational samples. The ATNF Pulsar Catalogue is a multifrequency, multifacility compilation, rather than a complete survey at a fixed sensitivity. Ideally, one would use a complete survey using FAST itself to judge the surface density of pulsars specifically at the detected flux density and band. Although this is not yet available, simulations[39] showed that FAST should able to discover about 1,000 pulsars, depending on the available observation time. This number is lower than what we have considered above using the whole ATNF catalogue, and does not change the previous conclusion.

Considering the reverse problem can be useful: we asked how many pulsars with magnetar behaviour there should be for an alignment with LS I +61° 303 to happen by chance. To do this, we simulated sets of Galactic positions of putative pulsars producing magnetar flares and measured the random coincidence between these and our source of interest (so that both sources lay within 3′). We did so with the spatial distribution of the current population of pulsars in Galactic longitude and latitude. Using 100,000 simulated sets (a larger number did not notably change the results), each with 1,928 magnetars, the average number of simulated coincidences between the position of one of them and LS I +61° 303 would be ~0.00093 (s.d. 0.0304). In this example, we took the actual number of known pulsars with $|b| < 5°$ (1,928) and considered that future samples will contain such a number of magnetars. This is indeed conservative. For context, this number is a factor of >60 beyond the magnetars known at present, a factor of 2 larger than all pulsars expected to be detected anew by FAST, or a factor of 4 larger than the number of magnetars born in the Galaxy in the last 25 kyr assuming the most favourable birth rate[52]. The main conclusion is that although it is formally impossible to rule out that a projected superposition of different sources, the combinations of these relatively rare systems in such a small region of the sky seems to be unlikely.

Data availability
The datasets generated during and/or analysed during the current study are available from the corresponding authors on reasonable request.

Code availability
PRESTO is available at https://www.cv.nrao.edu/~sransom/presto/ and BEAR is available at https://psr.pku.edu.cn/index.php/publications/software.

References
1. Dubus, G. Gamma-ray binaries and related systems. *Astron. Astrophys. Rev.* **21**, 64 (2013).
2. Abdo, A. A., Ackermann, M. & Ajello, M. et al. Fermi LAT observations of LS I +61 303: first detection of an orbital modulation in GeV gamma rays. *Astrophys. J. Lett.* **701**, L123–L128 (2009).
3. Gregory, P. C. Bayesian analysis of radio observations of the Be X-ray binary LS I +61 303. *Astrophys. J.* **575**, 427–434 (2002).
4. Albert, J., Aliu, E. & Anderhub, H. et al. Multiwavelength (radio, X-ray, and γ-ray) observations of the γ-ray binary LS I +61 303. *Astrophys. J.* **684**, 1351–1358 (2008).
5. Dhawan, V., Mioduszewski, A. & Rupen, M. LS I +61 303 is a Be-pulsar binary, not a microquasar. In *VI Microquasar Workshop: Microquasars and Beyond* 52.1 (ed. Belloni, T.) (Proceedings of Science, 2006).
6. Chernyakova, M. et al. Superorbital modulation of X-ray emission from gamma-ray binary LSI +61 303. *Astrophys. J. Lett.* **747**, L29 (2012).
7. Li, J., Torres, D. F. & Zhang, S. et al. Unveiling the super-orbital modulation of LS I +61 303 in X-Rays. *Astrophys. J. Lett.* **744**, L13 (2012).
8. Ackermann, M. et al. Associating long-term γ-ray variability with the superorbital period of LS I +61°303. *Astrophys. J. Lett.* **773**, L35 (2013).
9. Ahnen, M. L. et al. Super-orbital variability of LS I +61°303 at TeV energies. *Astron. Astrophys.* **591**, A76 (2016).

10. De Pasquale, M., Barthelmy, S. D. & Baumgartner, W. H. et al. Swift trigger 324362 (LS I +61 303 ?). *GRB Coord. Netw. Circ.* No. 8209 (2008).

11. Barthelmy, S. D. et al. Swift-BAT/-XRT refined analysis on trigger 324362 (LS I +61 303). *GRB Coord. Netw. Circ.* No. 8215 (2008).

12. Muñoz-Arjonilla, A. J. et al. Candidate counterparts to the soft gamma-ray flare in the direction of LS I +61 303. *Astron. Astrophys.* **497**, 457–461 (2009).

13. Torres, D. F., Rea, N. & Esposito, P. et al. A magnetar-like event from LS I +61 303 and its nature as a gamma-ray binary. *Astrophys. J.* **744**, 106 (2012).

14. Lindegren, L. et al. Gaia Early Data Release 3. The astrometric solution. *Astron. Astrophys.* **649**, A2 (2021).

15. Casares, J., Ribas, I., Paredes, J. M., Martí, J. & Allende Prieto, C. Orbital parameters of the microquasar LS I +61 303. *Mon. Not. R. Astron. Soc.* **360**, 1105–1109 (2005).

16. Grundstrom, E. D., Caballero-Nieves, S. M. & Gies, D. R. et al. Joint Hα and X-ray observations of massive x-ray binaries. II. The Be X-ray binary and microquasar LS I +61 303. *Astrophys. J.* **656**, 437–443 (2007).

17. Aragona, C. et al. The orbits of the γ-ray binaries LS I +61 303 and LS 5039. *Astrophys. J.* **698**, 514–518 (2009).

18. Massi, M. LS I +61°303 in the context of microquasars. *Astron. Astrophys.* **422**, 267–270 (2004).

19. Maraschi, L. & Treves, A. A model for LS I 61 303. *Mon. Not. R. Astron. Soc.* **194**, 1P–5P (1981).

20. Zamanov, R. K. An ejector-propeller model for LS I +61 303. *Mon. Not. R. Astron. Soc.* **272**, 308–310 (1995).

21. McSwain, M. V., Ray, P. S. & Ransom, S. M. et al. A radio pulsar search of the γ-ray binaries LS I +61 303 and LS 5039. *Astrophys. J.* **738**, 105 (2011).

22. Cañellas, A. et al. Search for radio pulsations in LS I +61 303. *Astron. Astrophys.* **543**, A122 (2012).

23. Rea, N., Torres, D. F. & van der Klis, M. et al. Deep Chandra observations of TeV binaries—I. LSI+61 303. *Mon. Not. R. Astron. Soc.* **405**, 2206–2214 (2010).

24. Hadasch, D., Torres, D. F. & Tanaka, T. et al. Long-term monitoring of the high-energy γ-ray emission from LS I +61 303 and LS 5039. *Astrophys. J.* **749**, 54 (2012).

25. Zdziarski, A. A., Neronov, A. & Chernyakova, M. A compact pulsar wind nebula model of the γ-ray-loud binary LS I +61°303. *Mon. Not. R. Astron. Soc.* **403**, 1873–1886 (2010).

26. Caliandro, G. A., Torres, D. F. & Rea, N. Impact of the orbital uncertainties on the timing of pulsars in binary systems. *Mon. Not. R. Astron. Soc.* **427**, 2251–2274 (2012).

27. Ransom, S. M., Eikenberry, S. S. & Middleditch, J. Fourier techniques for very long astrophysical time-series analysis. *Astron. J.* **124**, 1788–1809 (2002).

28. Yao, J. M., Manchester, R. N. & Wang, N. A new electron-density model for estimation of pulsar and FRB distances. *Astrophys. J.* **835**, 29 (2017).

29. Cordes, J. M. & Rickett, B. J. Diffractive interstellar scintillation timescales and velocities. *Astrophys. J.* **507**, 846–860 (1998).

30. Narayan, R. The physics of pulsar scintillation. *Phil. Trans. R. Soc. Lond. A* **341**, 151–165 (1992).

31. Sheikh, S. Z. & MacDonald, M. G. A statistical analysis of the nulling pulsar population. *Mon. Not. R. Astron. Soc.* **502**, 4669–4679 (2021).

32. Wang, N., Manchester, R. N. & Johnston, S. Pulsar nulling and mode changing. *Mon. Not. R. Astron. Soc.* **377**, 1383–1392 (2007).

33. McLaughlin, M. A. et al. Transient radio bursts from rotating neutron stars. *Nature* **439**, 817–820 (2006).

34. Johnston, S., Ball, L., Wang, N. & Manchester, R. N. Radio observations of PSR B1259-63 through the 2004 periastron passage. *Mon. Not. R. Astron. Soc.* **358**, 1069–1075 (2005).

35. Bogdanov, S. et al. Simultaneous Chandra and VLA observations of the transitional millisecond pulsar PSR J1023+0038: anti-correlated X-ray and radio variability. *Astrophys. J.* **856**, 54 (2018).

36. Papitto, A., Torres, D. F. & Rea, N. Possible changes of state and relevant timescales for a neutron star in LS I +61°303. *Astrophys. J.* **756**, 188 (2012).

37. Nan, R. et al. The Five-hundred-meter Aperture Spherical Radio Telescope (FAST) project. *Int. J. Mod. Phys. D* **20**, 989–1024 (2011).

38. Jiang, P. et al. Commissioning progress of the FAST. *Sci. China Phys. Mech. Astron.* **62**, 959502 (2019).

39. Han, J. L. et al. The FAST Galactic Plane Pulsar Snapshot survey: I. Project design and pulsar discoveries. *Res. Astron. Astrophys.* **21**, 107 (2021).

40. Qian, L. et al. FAST: its scientific achievements and prospects. *Innovation* **1**, 100053 (2020).

41. Pan, Z. et al. FAST Globular Cluster Pulsar survey: twenty-four pulsars discovered in 15 globular clusters. *Astrophys. J. Lett.* **915**, L28 (2021).

42. Lynch, R. S., Ransom, S. M., Freire, P. C. C. & Stairs, I. H. Six new recycled globular cluster pulsars discovered with the Green Bank Telescope. *Astrophys. J.* **734**, 89 (2011).

43. Men, Y. P. et al. Piggyback search for fast radio bursts using Nanshan 26 m and Kunming 40 m radio telescopes—I. Observing and data analysis systems, discovery of a mysterious peryton. *Mon. Not. R. Astron. Soc.* **488**, 3957–3971 (2019).

44. Lorimer, D. R. & Kramer, M. *Handbook of Pulsar Astronomy* (Cambridge Univ. Press, 2012).

45. Jiang, P. et al. The fundamental performance of FAST with 19-beam receiver at L band. *Res. Astron. Astrophys.* **20**, 064 (2020).

46. Lang, K. R. Interstellar scintillation of pulsar radiation. *Astrophys. J.* **164**, 249 (1971).

47. Romani, R. W., Narayan, R. & Blandford, R. Refractive effects in pulsar scintillation. *Mon. Not. R. Astron. Soc.* **220**, 19–49 (1986).

48. Bansal, K., Taylor, G. B., Stovall, K. & Dowell, J. Scattering study of pulsars below 100 MHz using LWA1. *Astrophys. J.* **875**, 146 (2019).

49. Kravtsov, V. et al. Orbital variability of the optical linear polarization of the γ-ray binary LS I +61° 303 and new constraints on the orbital parameters. *Astron. Astrophys.* **643**, A170 (2020).

50. Manchester, R. N., Hobbs, G. B., Teoh, A. & Hobbs, M. The Australia Telescope National Facility pulsar catalogue. *Astron. J.* **129**, 1993–2006 (2005).

51. Kaspi, V. M. & Beloborodov, A. M. Magnetars. *Annu. Rev. Astron. Astrophys.* **55**, 261–301 (2017).

52. Beniamini, P., Hotokezaka, K., van der Horst, A. & Kouveliotou, C. Formation rates and evolution histories of magnetars. *Mon. Not. R. Astron. Soc.* **487**, 1426–1438 (2019).

Author contributions

S.-S.W. proposed the observational project. The FAST team led by P.J. designed and scheduled the observations during the FAST commissioning stage. L.Q. carried out the observations and B.J.-W. analysed the data. D.F.T., J.L. and A.P. contributed to interpreting the results. D.F.T., S.-S.W. and B.-J.W. wrote the paper. P.J., R.X., J.-Z.Y., Q.-Z.L., M.-Y.G. and Q.-R.Y. participated in the interpretation of the results. All authors discussed the contents of the paper and contributed to the preparation of the manuscript.

Competing interests

The authors declare no competing interests.

Additional information

Supplementary information The online version contains supplementary material available at https://doi.org/10.1038/s41550-022-01630-1.

Correspondence and requests for materials should be addressed to Shan-Shan Weng or D. F. Torres.

Peer review information *Nature Astronomy* thanks Jumpei Takata, Scott Ransom and the other, anonymous, reviewer(s) for their contribution to the peer review of this work.

Reprints and permissions information is available at www.nature.com/reprints.

Publisher's note Springer Nature remains neutral with regard to jurisdictional claims in published maps and institutional affiliations.